Supporting Information

Structural Polymorphism of Alzheimer's β-Amyloid Fibrils as Controlled by an E22 Switch: A Solid-State NMR Study

Matthew R. Elkins [1$], Tuo Wang [1$], Mimi Nick [2], Hyunil Jo [2], Thomas Lemmin [2], Stanley B. Prusiner [3], William F. DeGrado [2], Jan Stöhr [3] and Mei Hong [1*]

[1] Department of Chemistry, Massachusetts Institute of Technology, Cambridge, MA 02139

[2] Department of Pharmaceutical Chemistry, University of California, San Francisco, San Francisco, CA 94158

[3] Institute for Neurodegenerative Diseases, Department of Neurology, University of California, San Francisco, San Francisco, CA 94143

[$] These authors contributed equally to this work.

* Corresponding author: Mei Hong, Email: meihong@mit.edu

Table S1. ^{13}C and ^{15}N chemical shifts (ppm) of the Arctic Aβ40 from 2D ^{13}C-^{13}C and ^{15}N-^{13}C correlation spectra. ^{15}N chemical shifts are referenced to liquid ammonia. All ^{13}C chemical shifts are referenced to DSS.

Site	^{15}N	C'	Cα	Cβ	Cγ/γ1	Cγ2	Cδ/Cδ1	Cδ2
F19 I	131.3	174.4	58.9	40.1	138.8		130.8/130.3	
F19 II	132.3	174.7	58.8	39.3				
A21 I	124.7	177.4	52.6	19.8				
A21 II	124.7	176.1	52.6	19.8				
A21 III	125.4	176.9	53.2	18.5				
I32 I	127.1	174.3	60.0	40.5	27.5	19.0	14.4	
I32 II	127.8	174.0	59.2	42.2	27.5	17.2	14.8	
I32 III	126.8	176.0	57.8	41.5	27.1	17.5	13.8	
I32 IV				42.7	26.5			
L34 I	111.5	178.3	56.3	42.2	27.5		26.1	20.9
L34 II	126.5	175.3	55.0	42.1	29.7		26.0	23.0
L34 III	121.2	176.2	55.1	45.6	27.0		25.8	
L34 IV			53.6	46.2	27.5			
V36 I	120.9	175.8	54.5	35.9	21.8	19.6		
V36 II	123.1	175.8	59.7	36.7	21.9	19.8		
V36 III	123.5	175.8	59.9	37.3	22.1	20.0		
G38 I	109.5	170.1	43.7					
G38 II	106.5	170.0	45.5					
G38 III	107.5	170.1	47.0					
G38 IV	105.0	171.1	46.1					

Table S2. ^{13}C and ^{15}N chemical shift (ppm) comparison of Arctic fibrils with other Aβ strains from literature. The Arctic chemical shifts are obtained from 50 ms ^{13}C-^{13}C DARR and ^{15}N-^{13}C HETCOR spectra. All ^{13}C chemical shifts are referenced to DSS and all ^{15}N chemical shifts are referenced to liquid ammonia.

Site	Reference	Aβ sample	^{15}N	C'	Cα	Cβ	Cγ/Cγ1	Cγ2	Cδ/Cδ1	Cδ2	Cε/Cε1	Cζ
F19	Petkova[1]	WT		171.9	56.5	42.6						
	Paravastu[2]	WT		173.0	56.4	42.5	138.5		131.0		130.0	127.3
	Lu[3]	WT	128.2	174.5	54.6	41.5	142.2		130.2			
	Elkins[4]	WT	130.1	172.6	56.2	42.9	139.2					
	Colvin[5]	WT42	130.4	174.4	59.9	40.3	139.6		130.5		129.7	
	Xiao[6]	WT42	130.2	174.9	60.8	41.1	139.7		130.5		130.5	128.0
	Elkins	Arctic I	131.3	174.4	58.9	40.1	138.8		130.8,130.3			
	Elkins	Arctic II	132.3	174.7	58.8	39.3						
	Schütz[7]	Osaka	129.5	174.2	55.6	42.4	142.6		130.6		131.5	128.9
	Elkins	Osaka DMSO	129.6	174.3	55.5	42.6	142.0		129.8			
	Elkins	Osaka NaOH	130.9	171.1	56.2	42.4	136.9		129.9			
A21	Petkova	WT		175.0	50.1	22.7						
	Paravastu	WT		175.4	50.0	22.4						
	Lu	WT	117.0	176.3	57.0	18.5						
	Elkins	WT	131.4	174.2	49.9	20.9						
	Colvin	WT-42	123.5	176.7	52.3	20.3						
	Xiao	WT-42	124.2	177.3	53.2	20.8						
	Elkins	Arctic I	124.7	177.4	52.6	19.8						
	Elkins	Arctic II	124.7	176.1	52.6	19.8						
	Elkins	Arctic III	125.4	176.9	53.2	18.5						
	Schütz	Osaka	115.1	177.2	49.0	23.2						
	Elkins	Osaka DMSO	114.9	177.4	49.0	23.2						
	Elkins	Osaka NaOH	128.9	172.7	49.6	19.4						

Site	Reference	Aβ sample	^{15}N	C'	Cα	Cβ	Cγ/Cγ1	Cγ2	Cδ/Cδ1	Cδ2	Cε/Cε1	Cζ
I32	Petkova	WT		174.8	58.2	42.4						
	Paravastu	WT		176.0	57.5	42.7	27.3	17.5	14.4			
	Lu	WT	124.7	175.9	58.5	41.1	27.1	16.5	14.7			
	Elkins	WT	126.7	176.6	57.9	41.8	27.2	17.8	15.1			
	Colvin	WT42	125.7	174.1	59.7	43.0	27.3	18.6	14.1			
	Xiao	WT42	126.5	174.3	60.3	41.5	27.8	18.7	14.4			
	Elkins	Arctic I	127.1	174.3	60.0	40.5	27.5	19.0	14.4			
	Elkins	Arctic II	127.8	174.0	59.2	42.2	27.5	17.2	14.8			
	Elkins	Arctic III	126.8	176.0	57.8	27.5	27.1	17.5	13.8			
	Schütz	Osaka	125.3	175.7	58.4	41.7	27.4	17.2	14.3			
	Elkins	Osaka DMSO	125.2	176.2	58.4	41.7	27.2	17.3	14.3			
	Elkins	Osaka NaOH	125.2	174.9	56.7	41.3	25.9	17.2	13.7,13.5			
L34	Petkova	WT		173.5	53.8	45.9						
	Paravastu	WT		173.5	54.5	46.1	27.5		25.4	23.1		
	Lu	WT	123.0	173.8	54.2	45.2	27.7		25.9	24.0		
	Elkins	WT	123.2	173.8	54.5	48.0	29.0		27.3	24.3		
	Colvin	WT42	110.7	178.3	56.7	41.7	27.1		26.0	20.9		
	Xiao	WT42	111.5	178.6	57.4	42.1	26.9		24.6	21.7		
	Elkins	Arctic I	111.5	178.3	56.3	42.2	27.5		26.1	20.9		
	Elkins	Arctic II	126.5	178.0	55.0	42.1	29.7		26.0	23.0		
	Schütz	Osaka	125.5	173.8	54.1	45.8	28.1		25.6	24.9		
	Elkins	Osaka DMSO	125.1	173.8	54.3	46.0	28.2		25.7	24.9		
	Elkins	Osaka NaOH	124.4	172.0	52.9	44.8	27.6		25.1	23.5		
V36	Petkova	WT	124.3	175.2	59.7	34.9						
	Paravastu	WT		174.6	59.4	34.9	20.9	19.4				
	Lu	WT	125.2	175.8	58.9	35.0	20.9	19.6				
	Elkins	WT	128.3	175.4	60.8	33.4	21.6	21.1				
	Elkins	WT II	128.0	175.8	67.6	29.0	24.1	22.7				

Site	Reference	Aβ sample	^{15}N	C'	Cα	Cβ	Cγ/Cγ1	Cγ2	Cδ/Cδ1	Cδ2	Cε/Cε1	Cζ
	Colvin	WT42	124.6	174.7	60.2	34.5	21.2	19.5				
	Xiao	WT42	124.4	175.2	60.9	34.8	21.7	19.9				
	Elkins	Arctic I	120.9	175.8	58.5	35.9	21.8	19.6				
	Elkins	Arctic II	123.1	175.8	59.7	36.7	21.9	19.8				
V36	Elkins	Arctic III	123.5	175.8	59.9	37.3	22.1	20.0				
	Schütz	Osaka	125.4	176.2	58.7	36.1	21.7					
	Elkins	Osaka DMSO	125.6	176.3	58.9	35.8	21.8	21.3				
	Elkins	Osaka NaOH	127.3	173.8	59.6	32.7	20.7	19.9				
	Petkova	WT	104.2	170.4	44.8							
	Paravastu	WT		171.1	45.0							
	Lu	WT	106.0	169.8	44.9							
	Elkins	WT	106.5	170.8	46.8							
	Colvin	WT42	110.8	174.3	48.2							
	Xiao	WT42	113.6	173.5	48.8							
G38	Elkins	Arctic I	109.5	170.1	43.7							
	Elkins	Arctic II	106.5	170.0	45.5							
	Elkins	Arctic III	107.5	170.1	47.0							
	Elkins	Arctic IV	105.0	171.1	46.1							
	Schütz	Osaka	105.7	169.8	45.0							
	Elkins	Osaka DMSO	105.8	169.9	45.0							
	Elkins	Osaka NaOH	104.7	170.3	44.0							

1. Petkova *et al*. 2006 – ^{13}C chemical shifts obtained from DSS-referenced values deposited for PDB accession code 2LMN [1].
2. Paravastu *et al.* 2008 – ^{13}C chemical shifts obtained by adding 2.0 ppm to TMS-referenced values in paper [2].
3. Lu *et al.* 2013 – ^{13}C chemical shifts obtained from DSS-referenced values in paper [3].
4. Elkins – ^{13}C chemical shifts referenced on the DSS scale.
5. Colvin *et al.* 2015 – ^{13}C chemical shifts obtained from DSS-referenced values in paper [4].
6. Xiao *et al.* 2015 – ^{13}C chemical shifts obtained by adding 2.0 ppm to TMS-referenced values in paper [5].
7. Schutz *et al.* 2015 – ^{13}C chemical shifts obtained from DSS-referenced values deposited for PDB accession code 2MVX [6].

Table S3. ^{1}H $T_{1\rho}$ relaxation times of Aβ samples measured with a 62.5 kHz spin-lock field. The curves are fit using single and double exponential functions $I(t) = e^{-t/T_{1\rho,b}}$ and $I(t) = ae^{-t/T_{1\rho,a}} + be^{-t/T_{1\rho,b}}$, where b = 1-a. . ^{13}C chemical shifts are referenced to DSS.

Arctic DMSO, 298 K					
Carbon	δ (ppm)	$T_{1\rho,a}$ (ms)	$T_{1\rho,b}$ (ms)	*a*	*b*
F19I32V36a	59.0	2.9±0.6	47±3	0.22±0.22	0.78±0.22
F19b	40.1	3.1±0.7	42±3	0.23±0.03	0.77±0.03
F19R	130.9	5±3	35±10	0.49±0.18	0.51±0.18
A21a	52.7	2.5±0.5	24±1	0.18±0.02	0.82±0.02
I32d	14.7		68±2		1
L34a	55.0	4.2±0.6	47±4	0.35±0.03	0.65±0.03
L34d2	23.0	5±1	88±9	0.15±0.02	0.85±0.02
V36a/I32a	59.7	2.9±0.5	39±2	0.28±0.02	0.72±0.02
V36b	49.2	1.1±0.2	52±2	0.14±0.86	0.86±0.86
Arctic DMSO, 260 K					
Carbon	δ (ppm)	$T_{1\rho,a}$ (ms)	$T_{1\rho,b}$ (ms)	a	b
F19I32V36a	59.0	1.6±0.3	31±1	0.18±0.01	0.82±0.01
F19b	40.1	2.2±0.4	28±2	0.31±0.03	0.69±0.03
F19R	130.9	0.9±0.1	15±2	0.48±0.03	0.52±0.03
A21a	52.7	3±1	27±4	0.35±0.07	0.65±0.07
I32d	14.7	13±5	82±84	0.61±0.25	0.39±0.25
L34a	55.0	3.0±0.5	34±3	0.31±0.03	0.69±0.03
L34d2	23.0	9±3	60±38	0.58±0.18	0.42±0.18
V36a/I32a	59.7	2.5±0.5	30±2	0.26±0.03	0.74±0.03
V36b	49.2	2.4±0.3	40±2	0.28±0.01	0.72±0.01
Wild type, DMSO, 298 K					
Carbon	δ (ppm)	$T_{1\rho,a}$ (ms)	$T_{1\rho,b}$ (ms)	a	b
F19a	56.0	1.7±0.4	14±1	0.27±0.04	0.73±0.04
F19b	42.9	3.0±0.5	25±4	0.53±0.06	0.47±0.06
F19R	132.6	1.2±0.2	14±3	0.66±0.05	0.34±0.05
A21a	49.9	4±1	23±3	0.37±0.09	0.63±0.09
I32d	15.2	6±1	34±8	0.56±0.09	0.44±0.09
L34a	54.5	2.5±0.6	52±4	0.22±0.02	0.78±0.02
L34d2/V36g2	24.4	3.3±0.3	44±3	0.41±0.02	0.59±0.02
V36a	60.8	3.2±0.4	38±4	0.45±0.03	0.55±0.03
V36b	33.5	1.8±0.4	35±5	0.46±0.04	0.54±0.04
Wild type, DMSO, 260 K					
Carbon	δ (ppm)	$T_{1\rho,a}$ (ms)	$T_{1\rho,b}$ (ms)	a	b
F19a	56.0	1.6±0.5	30±2	0.18±0.02	0.82±0.02
F19b	42.9	5.1±0.8	45±4	0.36±0.04	0.64±0.04
F19R	132.6	2.9±0.2	41±8	0.65±0.02	0.35±0.02
A21a	49.9	5±2	40±6	0.24±0.07	0.76±0.07
I32d	15.2		61±5		1
L34a	54.5	0.7±0.2	89±6	0.14±0.01	0.86±0.01
L34d2/V36g2	24.4		81±2		1
V36a	60.8	2.2±0.4	37±3	0.31±0.03	0.69±0.03
V36b	33.5	6±1	54±11	0.50±0.06	0.50±0.06
Osaka DMSO, 298 K					

Carbon	δ (ppm)	$T_{1\rho, a}$ (ms)	$T_{1\rho, b}$ (ms)	a	b
F19a	55.6	4.2±0.4	26±2	0.47±0.03	0.53±0.03
F19b	42.6	3.6±0.3	29±2	0.48±0.02	0.52±0.02
F19R	131.5	0.7±0.1	13±1	0.42±0.03	0.58±0.03
A21a	49.2		28±1		1
I32d	14.5	3±4	36±3	0.25±0.04	0.75±0.04
L34a	54.3	6.2±0.7	39±4	0.48±0.04	0.52±0.04
L34d2	24.9	1.2±0.3	49±2	0.17±0.01	0.83±0.01
V36a/I32a	58.6	4±1	51±3	0.16±0.02	0.84±0.02
V36b	36.2	2±1	60±4	0.11±0.02	0.89±0.02
Osaka DMSO, 260 K					
Carbon	δ (ppm)	$T_{1\rho, a}$ (ms)	$T_{1\rho, b}$ (ms)	a	b
F19a	55.6	3.2±0.9	38±2	0.20±0.03	0.80±0.03
F19b	42.6	2.1±0.4	31±1	0.18±0.02	0.82±0.02
F19R	131.5	2.0±0.3	32±2	0.32±0.02	0.68±0.03
A21a	49.2		30±1		1
I32d	14.5	3.0±0.9	27±3	0.33±0.06	0.67±0.06
L34a	54.3	7±1	41±3	0.24±0.04	0.76±0.04
L34d2	24.9	0.8±0.2	35±2	0.19±0.02	0.81±0.02
V36a/I32a	58.6	6±2	49±3	0.17±0.03	0.83±0.03
V36b	36.2	2.0±0.8	47±3	0.13±0.02	0.87±0.02

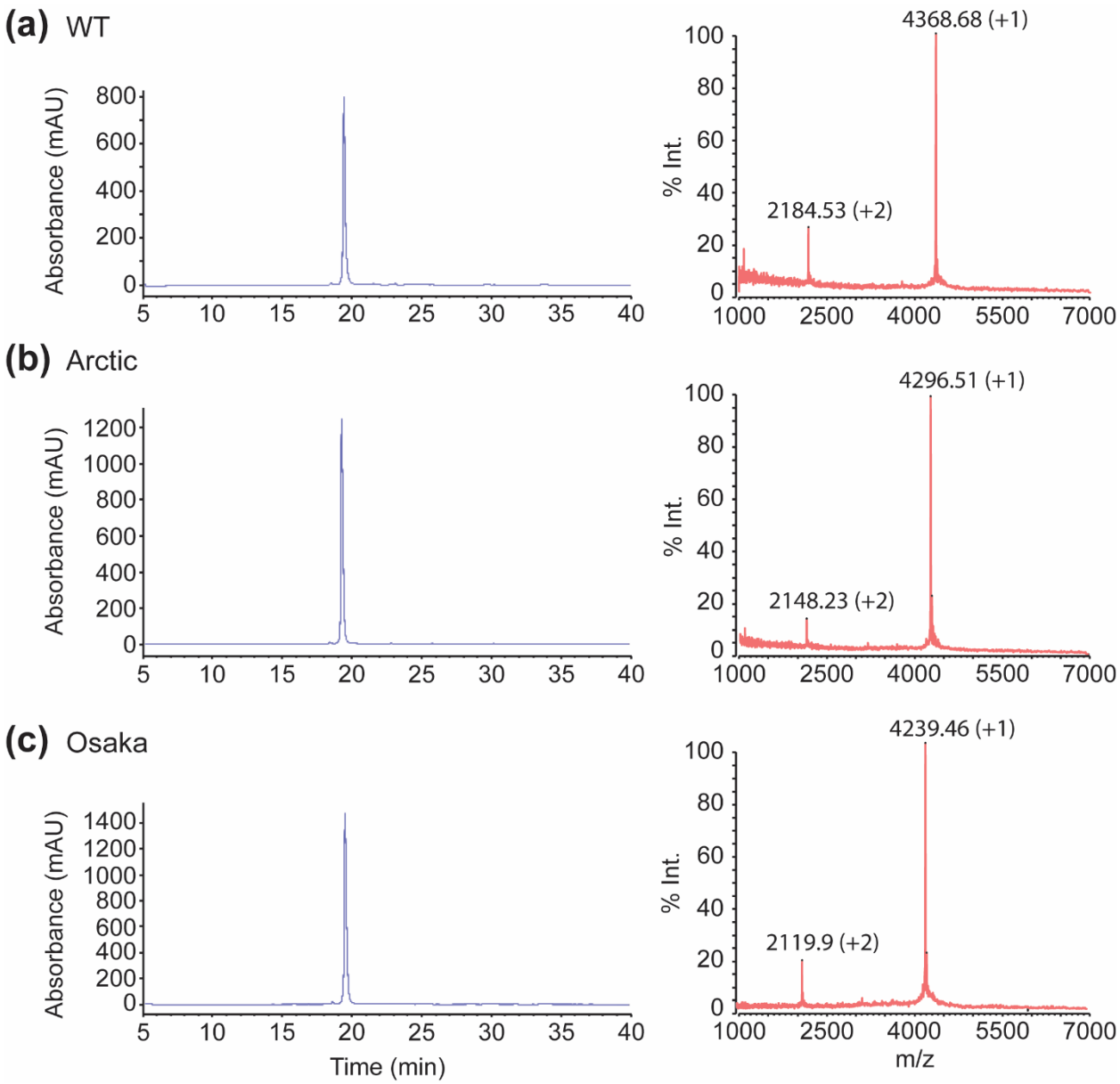

Figure S1. HPLC profiles and MALDI spectra of isotopically labeled Aβ. (a) WT Aβ40; (b) Arctic E22G Aβ40; (c) Osaka E22Δ Aβ40. The purity of all the peptides were >95% based upon HPLC by absorbance at 220 nm. Typically 15-20 mg of the purified peptides were obtained after extensive HPLC of the crude product (app. 250 mg, 55% crude yield) in 0.1 mmol scale synthesis.

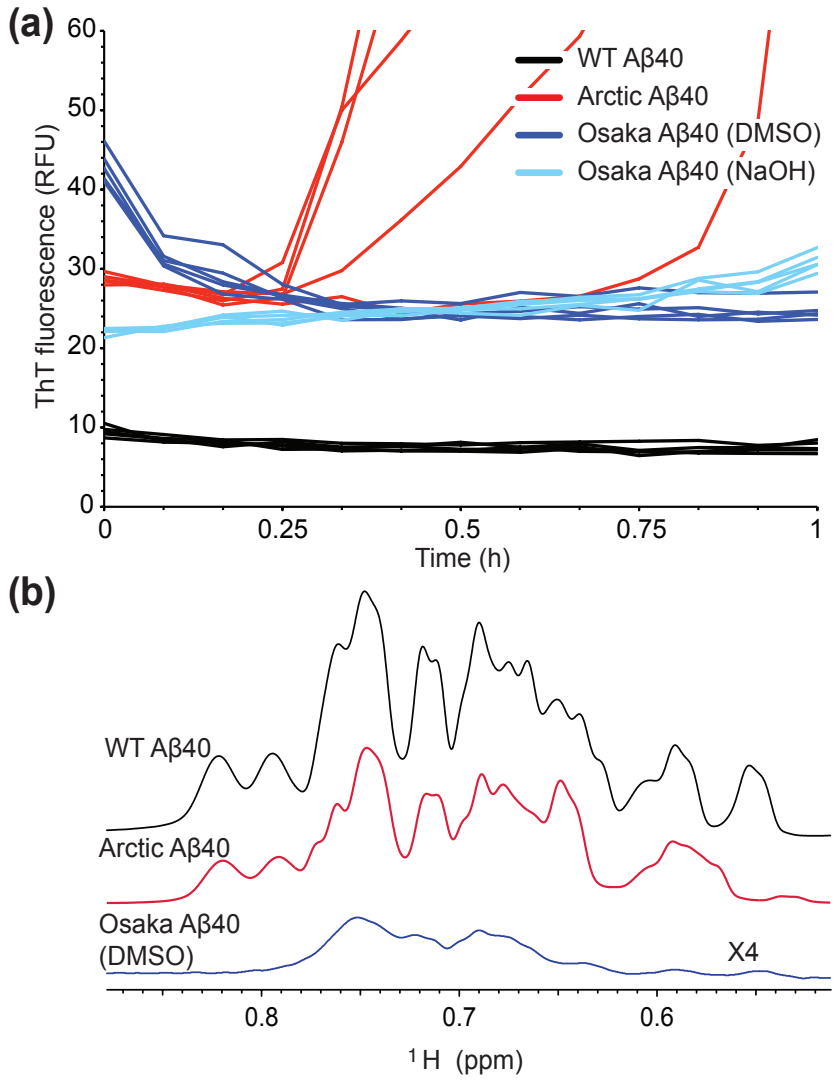

Figure S2. Early time points of fibrillization. (a) Kinetics of fibril formation (0.2 mg/ml in 10 mM sodium phosphate buffer, pH 7.2) were measured by the amyloid-binding dye ThT (10 μM). n=5 (b) Formation of insoluble fibrils by WT, Arctic, and Osaka Aβ40 peptides (0.2 mg/ml) was observed by disappearance of methyl group signals in ^{1}H solution NMR spectra, which were recorded 5 minutes after sample preparation. The starting concentrations for all samples were 100 μ M. The spectra were recorded with 256 scans at 295 K on a Bruker Avance II 900 MHz spectrometer.

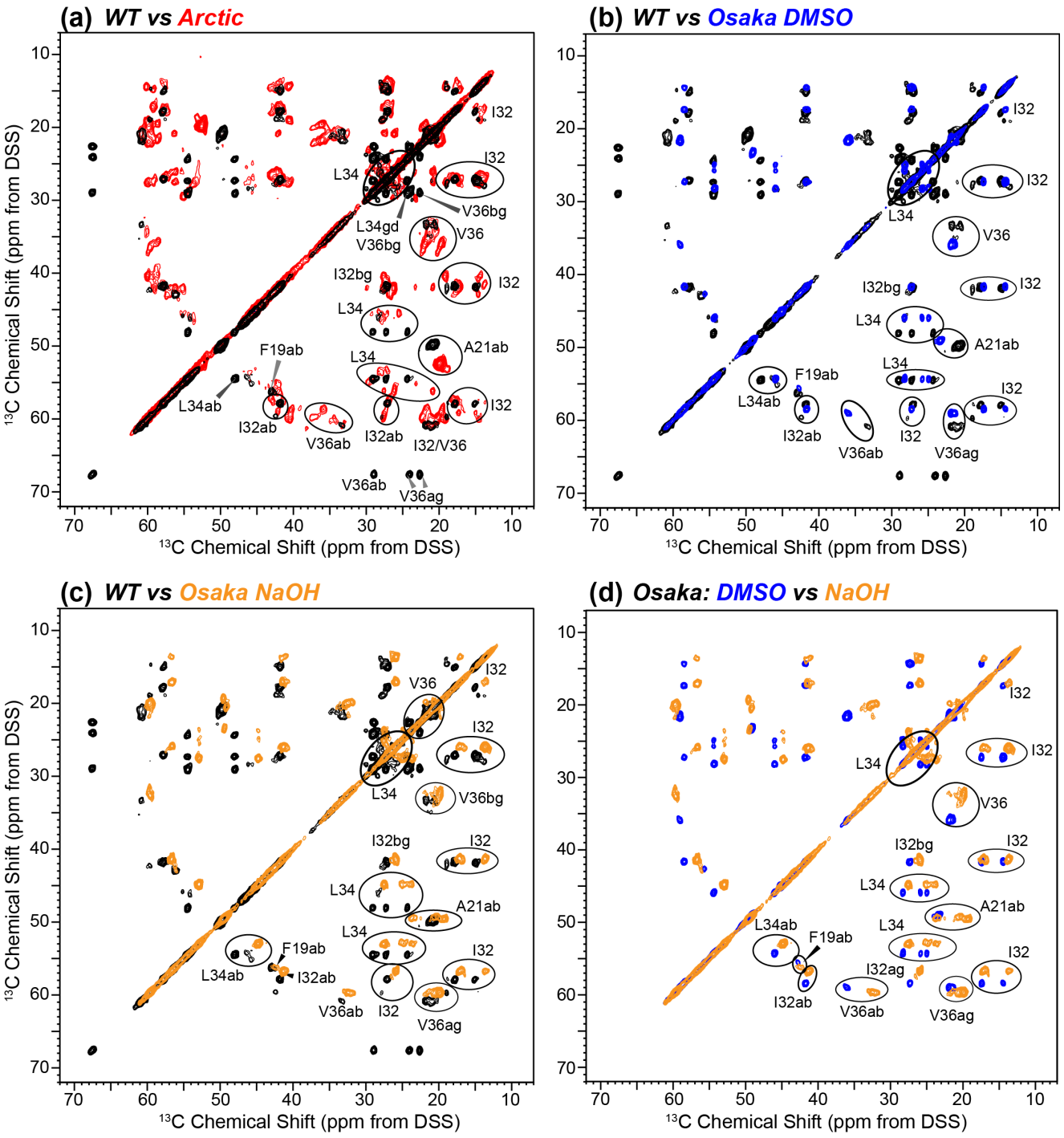

Figure S3. Pairwise overlays of 50 ms 2D ^{13}C-^{13}C DARR spectra of four Aβ40 fibril samples indicate chemical shift differences. The WT, Arctic, Osaka DMSO and Osaka NaOH spectra are shown in black, red, blue and orange, respectively. (a) WT and Arctic Aβ40 spectra. (b) WT and Osaka DMSO Aβ40 spectra. (c) WT and Osaka NaOH Aβ40 spectra. (d) Osaka DMSO and Osaka NaOH spectra.

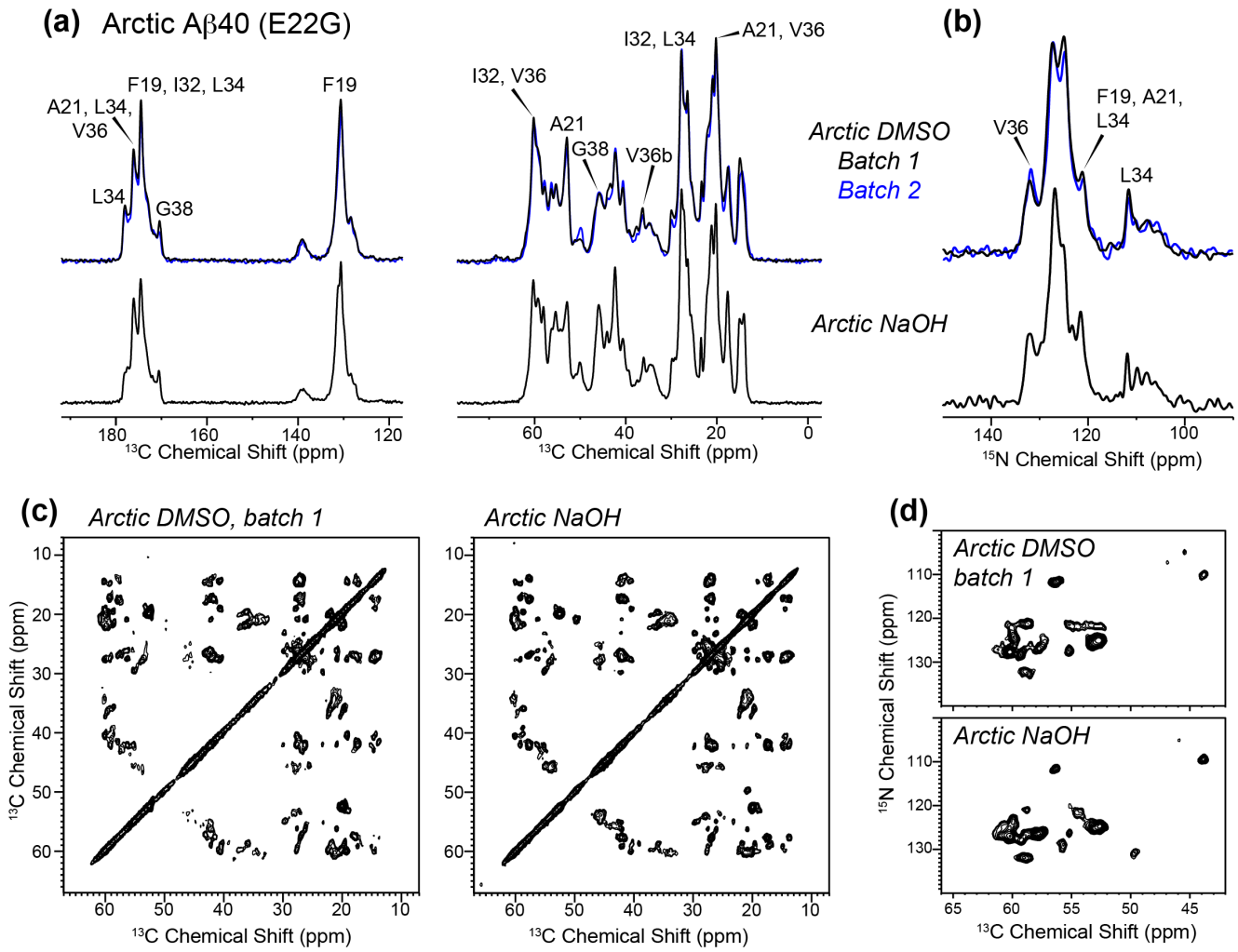

Figure S4. Batch-to-batch peptide reproducibility and solvent independence of the Arctic Aβ40 fibrils. (a) 1D ^{13}C CP spectra and (b) 1D ^{15}N CP spectra of Arctic Aβ40 fibrils prepared in DMSO (top trace) and NaOH (bottom trace). For the DMSO condition, two batches of peptides were synthesized and fibrilized, with no observable spectral differences, confirming that the molecular structural polymorphism is reproducible and intrinsic to this sequence. (c) 50 ms 2D ^{13}C-^{13}C and (d) 2D ^{15}N-^{13}C correlation spectra of Arctic DMSO (batch 1) and Arctic NaOH fibrils. The two spectra are similar, indicating that the solvent condition has little effect on the fibril structure in the case of Arctic Aβ40, which differs from the behavior of Osaka Aβ40 fibrils.

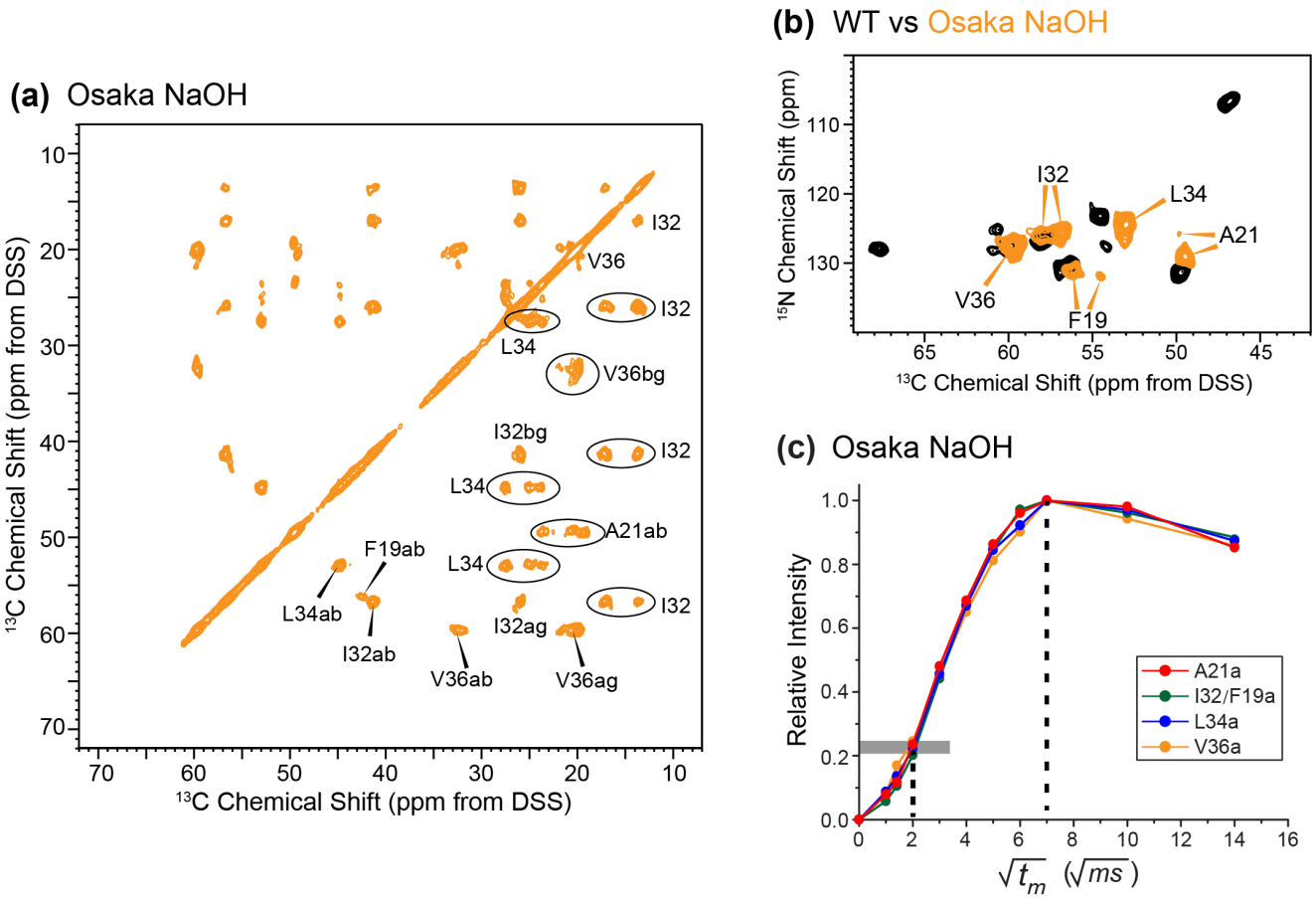

Figure S5. Additional NMR data of Osaka NaOH Aβ40 fibrils. (a) 50 ms 2D ^{13}C-^{13}C DARR spectrum with 50 ms mixing. (b) 2D ^{15}N-^{13}C correlation spectrum. (c) Water-to-protein ^{1}H spin diffusion buildup curves.

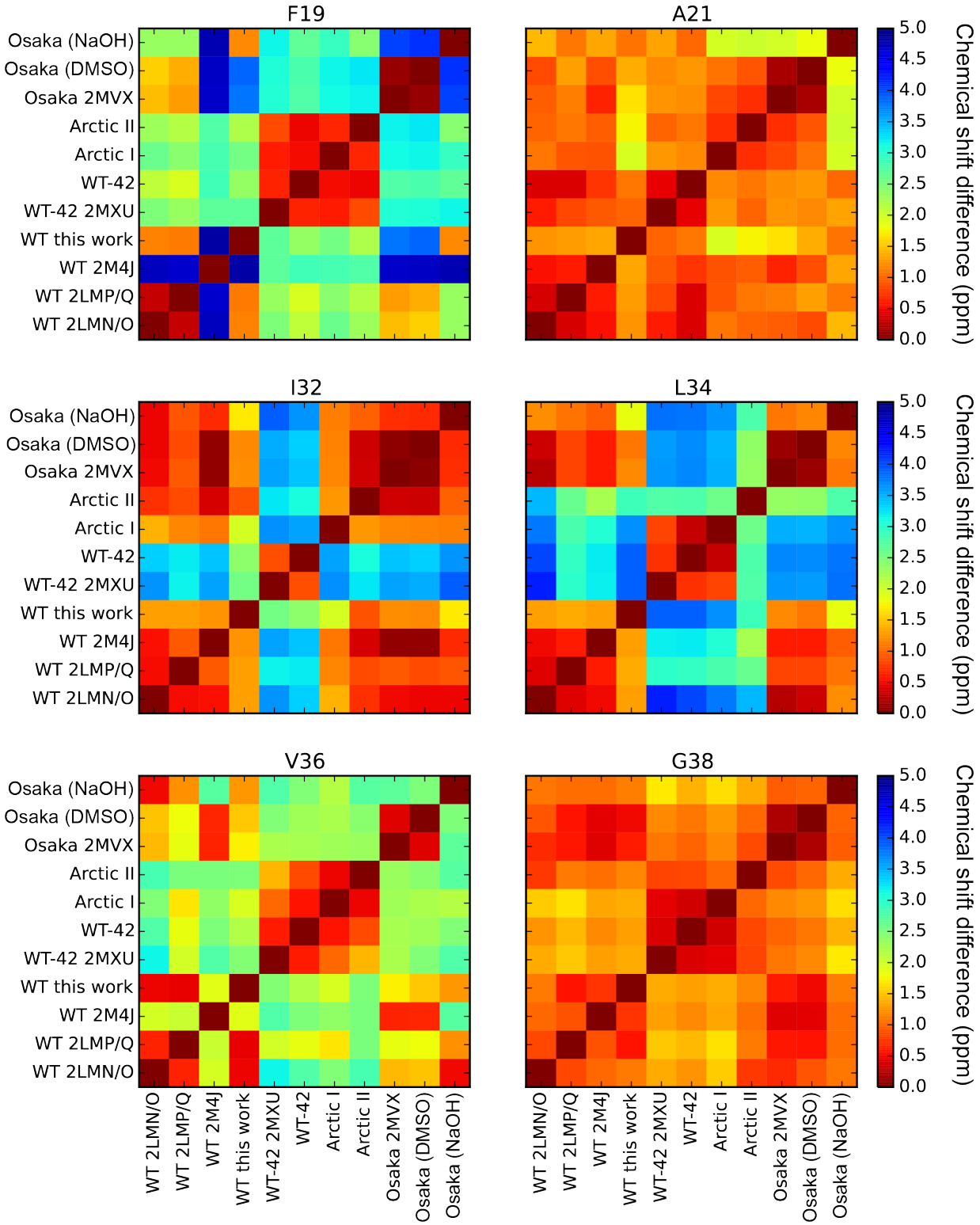

Figure S6. Residue-specific heat maps representing the pairwise Pearson correlation coefficients between the chemical shifts of different Aβ strains studied here and reported in the literature.

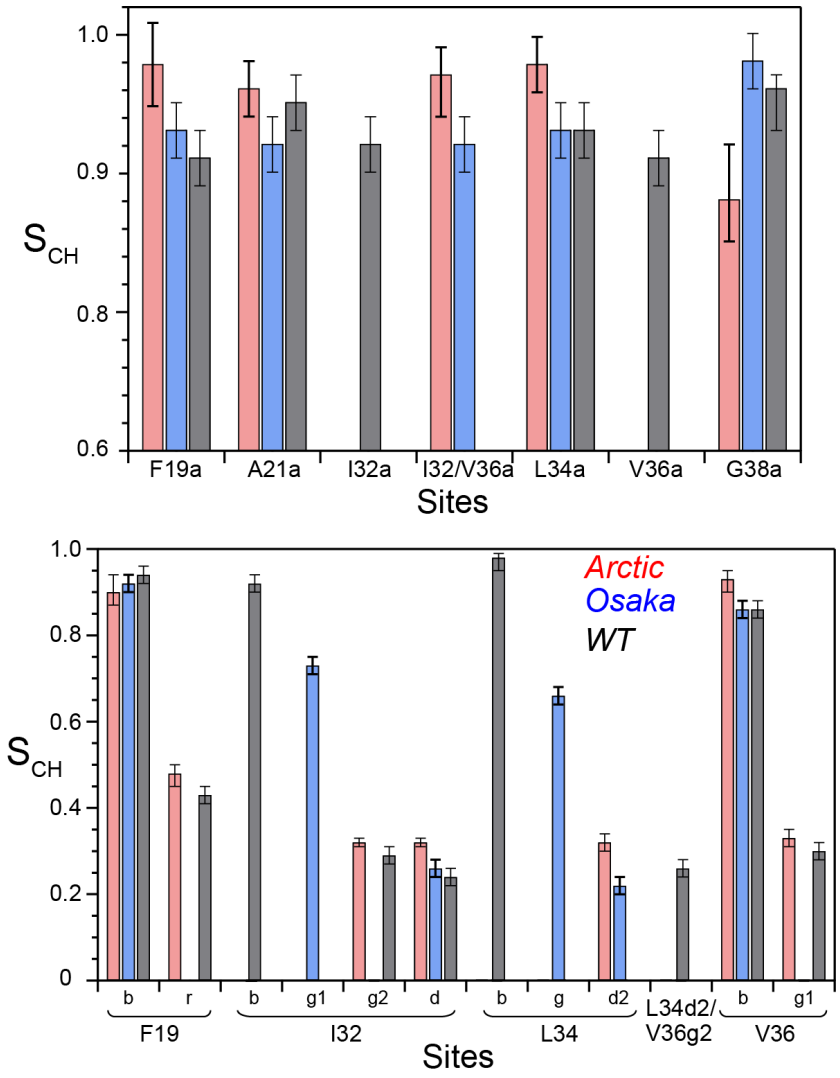

Figure S7. C-H dipolar order parameters S_{CH} of Arctic, WT and Osaka DMSO Aβ40 fibrils for backbone Cα (top) and sidechain (bottom) carbons.

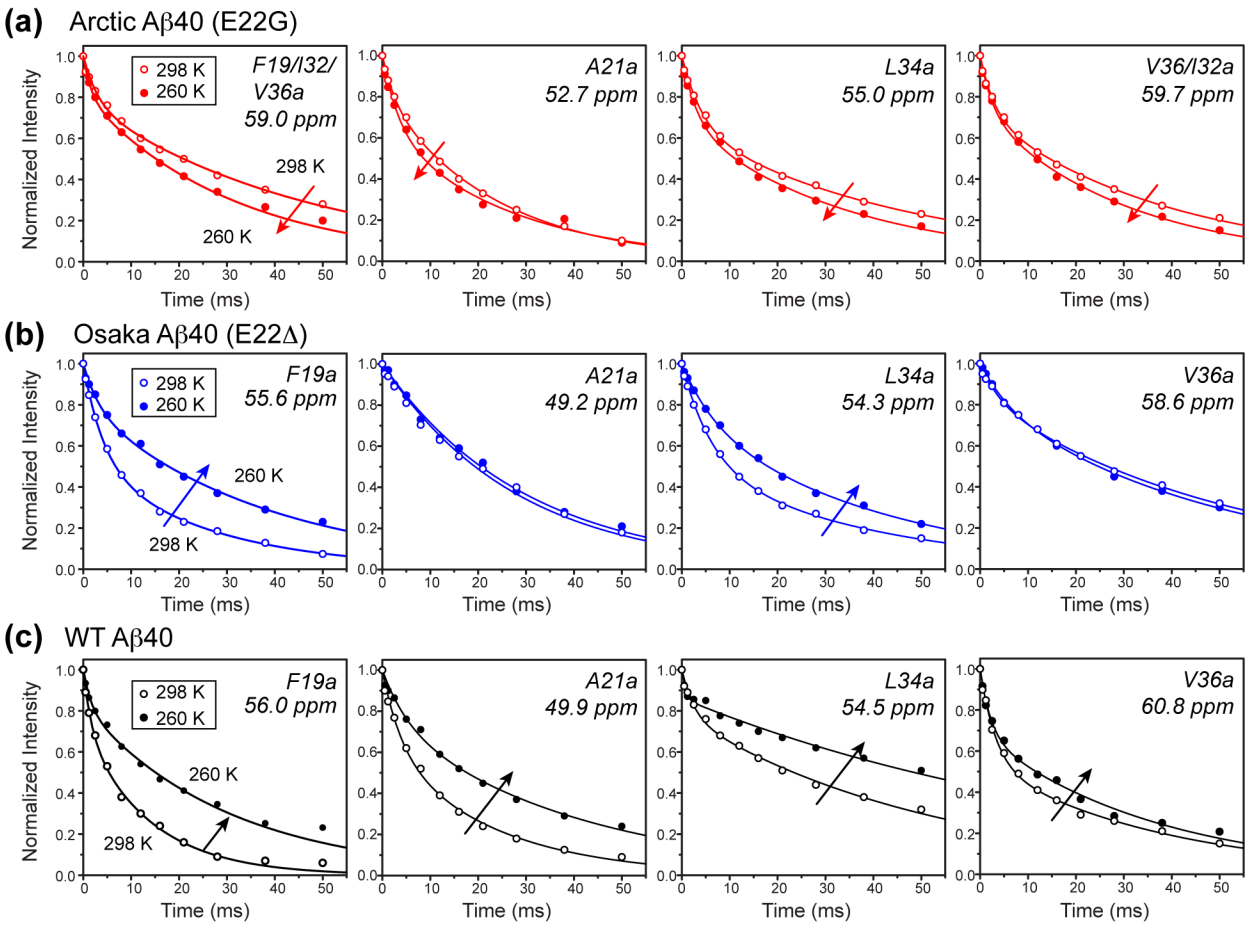

Figure S8. Temperature dependence of ^{1}H $T_{1\rho}$ relaxation times of backbone Cα sites in (a) Arctic, (b) Osaka DMSO, and (c) WT Aβ40. Both Arctic and Osaka Aβ40 have similar ^{1}H $T_{1\rho}$ values between 298 K and 260 K, while the WT peptide shows much longer $T_{1\rho}$ with decreasing temperature. This indicates that at ambient temperature, the microsecond motions are slower in WT Aβ40 than in Arctic and Osaka Aβ40.

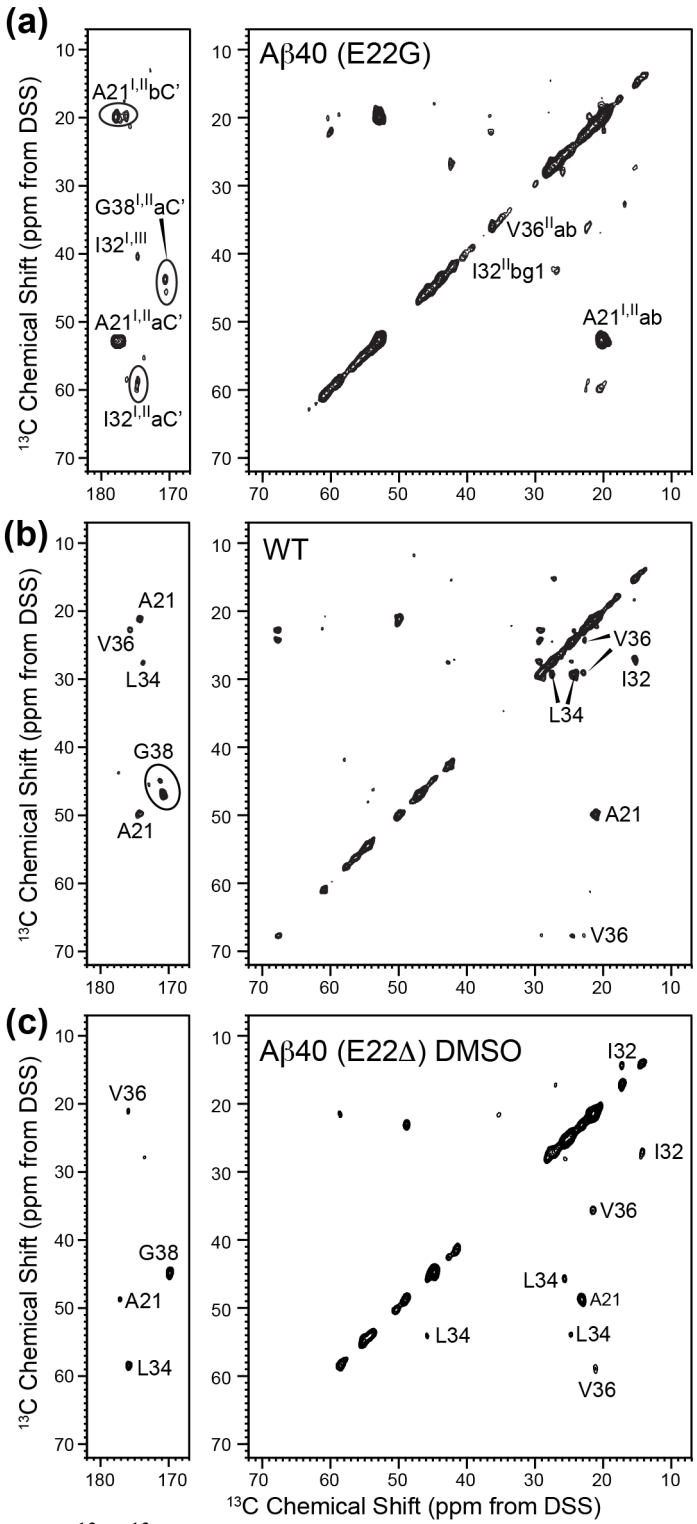

Figure S9. Water-edited 2D ^{13}C-^{13}C DARR spectra of (a) Arctic Aβ, (b) wild type Aβ40, and (c) Osaka Aβ40. The spectra were measured at 277 K under 10.5 kHz. The ^{1}H T_2 filter time was 600 μs and the ^{1}H spin diffusion mixing period was 4 ms. All spectra are plotted using Topspin parameters of lev0 = 4, toplev = 90 and nlev =16.

References

(1) Petkova, A. T.; Yau, W. M.; Tycko, R. *Biochemistry* **2006**, *45*, 498-512.
(2) Paravastu, A. K.; Leapman, R. D.; Yau, W. M.; Tycko, R. *Proc. Natl. Acad. Sci. USA* **2008**, *105*, 18349-18354.
(3) Lu, J. X.; Qiang, W.; Yau, W. M.; Schwieters, C. D.; Meredith, S. C.; Tycko, R. *Cell* **2013**, *154*, 1257-1268.
(4) Colvin, M. T.; Silvers, R.; Frohm, B.; Su, Y.; Linse, S.; Griffin, R. G. *J. Am. Chem. Soc.* **2015**, *137*, 7509-7518.
(5) Xiao, Y. L.; Ma, B. Y.; McElheny, D.; Parthasarathy, S.; Long, F.; Hoshi, M.; Nussinov, R.; Ishii, Y. *Nat. Struct. Mol. Biol.* **2015**, *22*, 499-U497.
(6) Schutz, A. K.; Vagt, T.; Huber, M.; Ovchinnikova, O. Y.; Cadalbert, R.; Wall, J.; Guntert, P.; Bockmann, A.; Glockshuber, R.; Meier, B. H. *Angew. Chem. Int. Ed. Engl.* **2015**, *54*, 331-335.